

1 **Xylosyltransferase Bump-and-hole Engineering to Chemically Manipulate**  
2 **Proteoglycans in Mammalian Cells**

3  
4 Zhen Li<sup>a,b</sup>, Lucia Di Vagno<sup>b,c</sup>, Aisling Ni Cheallaigh<sup>d</sup>, Douglas Sammon<sup>e</sup>, David C. Briggs<sup>f</sup>,  
5 Nara Chung<sup>g</sup>, Vincent Chang<sup>g</sup>, Keira E. Mahoney<sup>g</sup>, Anna Cioce<sup>a,b</sup>, Lloyd D. Murphy<sup>h</sup>, Yen-Hsi  
6 Chen<sup>i,j</sup>, Yoshiki Narimatsu<sup>i</sup>, Rebecca L. Miller<sup>i</sup>, Lianne I. Willems<sup>h</sup>, Stacy A. Malaker<sup>g</sup>, Gavin  
7 J. Miller<sup>d</sup>, Erhard Hohenester<sup>e</sup>, Benjamin Schumann<sup>a,b</sup>

8  
9 <sup>a</sup> Department of Chemistry, Imperial College London, W12 0BZ, London, United Kingdom.

10 <sup>b</sup> Chemical Glycobiology Laboratory, The Francis Crick Institute, NW1 1AT London, United  
11 Kingdom

12 <sup>c</sup> Proteomics Science Technology Platform, The Francis Crick Institute, London NW1 1AT,  
13 United Kingdom.

14 <sup>d</sup> Lennard-Jones Laboratory, School of Chemical & Physical Sciences, and Centre for  
15 Glycoscience, Keele University, Keele, Staffordshire, ST5 5BG United Kingdom

16 <sup>e</sup> Department of Life Sciences, Imperial College London, London SW7 2AZ, UK.

17 <sup>f</sup> Signalling and Structural Biology Laboratory, The Francis Crick Institute, London NW1 1AT,  
18 United Kingdom.

19 <sup>g</sup> Department of Chemistry, Yale University, CT 06511, New Haven, United States.

20 <sup>h</sup> York Structural Biology Laboratory and York Biomedical Research Institute, Department of  
21 Chemistry, University of York, York YO10 5DD, United Kingdom

22 <sup>i</sup> Copenhagen Center for Glycomics, Department of Cellular and Molecular Medicine, Faculty  
23 of Health Sciences, University of Copenhagen; Copenhagen-N, Denmark.

24 <sup>j</sup> Current address: GlycoDisplay ApS, Copenhagen, Denmark.

25

26 **Abstract**

27 Mammalian cells orchestrate signalling through interaction events on their surfaces.  
28 Proteoglycans are an intricate part of these interactions, carrying large glycosaminoglycan  
29 polysaccharides that recruit signalling molecules. Despite their importance in development,  
30 cancer and neurobiology, a relatively small number of proteoglycans have been identified. In  
31 addition to the complexity of glycan extension, biosynthetic redundancy in the first protein  
32 glycosylation step by two xylosyltransferase isoenzymes XT1 and XT2 complicates  
33 annotation of proteoglycans. Here, we develop a chemical strategy that allows profiling of  
34 cellular proteoglycans. By employing a tactic termed bump-and-hole engineering, we  
35 engineer the two isoenzymes XT1 and XT2 to specifically transfer a chemically modified  
36 xylose analogue to target proteins. The chemical modification contains a bioorthogonal tag,  
37 allowing the ability to visualise and profile target proteins modified by both transferases in

1 mammalian cells as well as pinpointing glycosylation sites by mass spectrometry.  
2 Engineered XT enzymes permit a view into proteoglycan biology that is orthogonal to  
3 conventional techniques in biochemistry.

4

5 **Main**

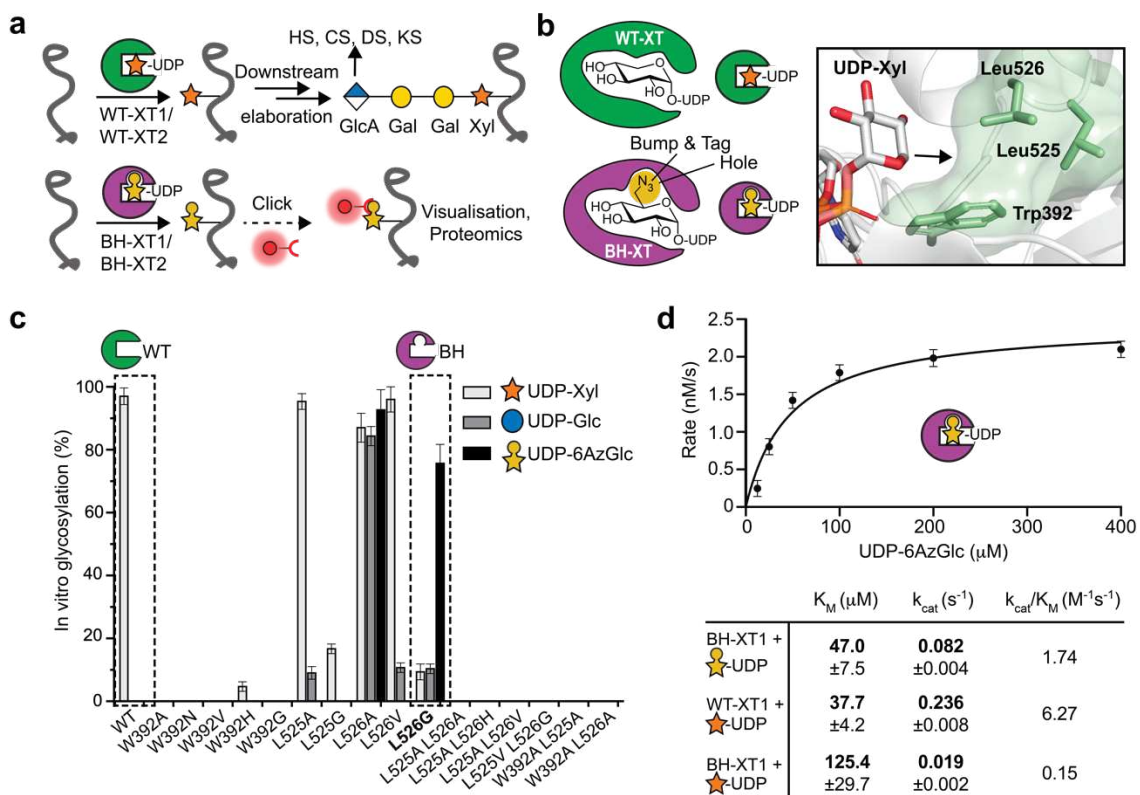
6 Proteoglycans are large biomolecules that consist of a core protein and one or more  
7 glycosaminoglycan (GAG) modifications. Ubiquitous on cell surfaces and within the  
8 extracellular matrix in higher eukaryotes, proteoglycans form a myriad of interactions with  
9 cellular receptors as well as soluble signalling molecules, and provide structural support in  
10 connective tissues such as cartilage.<sup>1,2</sup> Growth factors, neurotrophic factors and chemokines  
11 can be recruited to target cells through GAG binding sites, rendering proteoglycans  
12 important determinants for development.<sup>3,4</sup> Consequently, dysfunctions in GAG biosynthesis  
13 cause severe phenotypes from embryonic lethality to skeletal and muscular deficiencies.<sup>5</sup>  
14 Binding events between proteoglycans and their receptors are impacted by the core protein  
15 as well as the identity of GAG polysaccharides that are classified into either heparan sulfate  
16 (HS), chondroitin sulfate (CS), dermatan sulfate (DS) or keratan sulfate (KS).<sup>6,7</sup> Biochemistry  
17 and genetic engineering have linked proteoglycan physiology to the GAG structures on  
18 particular cell types or even on distinct subcellular locations.<sup>8–13</sup> Despite their relevance in  
19 physiology, only a relatively small number of less than 50 proteoglycans is known in  
20 humans.<sup>14,15</sup>

21

22 An impediment for the identification of proteoglycans is the large size of GAG modifications  
23 that renders analysis by mass spectrometry (MS) challenging. While GAG-carrying  
24 glycopeptides contain common amino acid signatures such as acidic patches and a central  
25 O-glycosylated Ser with often flanking Gly or Ala residues, there is no consensus sequence  
26 to predict GAG glycosylation in the Golgi.<sup>6,9,16,17</sup> Common strategies to identify proteoglycans  
27 feature enzymatic digestion of GAG chains either before or after isolation of  
28 glycopeptides.<sup>9,18–23</sup> While powerful, such procedures make use of complex digestion and  
29 purification protocols and focus solely on the GAG-carrying glycopeptide, without the  
30 advantages of shotgun (glyco-)proteomics methods that employ the full MS peptide  
31 coverage of individual proteins for detection.

32

33



1  
2 **Fig. 1:** Design of a xylosyltransferase bump-and-hole system. **a**, principle of the BH approach. WT-  
3 XTs transfer Xyl to substrate proteins that can be extended to GAG chains. BH-XTs transfer a  
4 bioorthogonal Xyl analogue for visualisation and MS profiling. **b**, structural considerations of XT1  
5 engineering to accept UDP-6AzGlc instead of UDP-Xyl. Insert: Gatekeeper residues in the XT1  
6 crystal structure (PDB 6EJ7) and structural trajectory of 6-azidomethyl modification in UDP-6AzGlc. **c**,  
7 *in vitro* glycosylation of a fluorescently labelled bikunin substrate peptide by WT- or mutant XT1 and  
8 different UDP-sugars. Data are means ± SD from three technical replicates from one out of two  
9 independent experiments. **d**, Michaelis-Menten kinetics of *in vitro* peptide glycosylation by different  
10 XT1/UDP-sugar combinations. Data are means ± SD from three technical replicates.

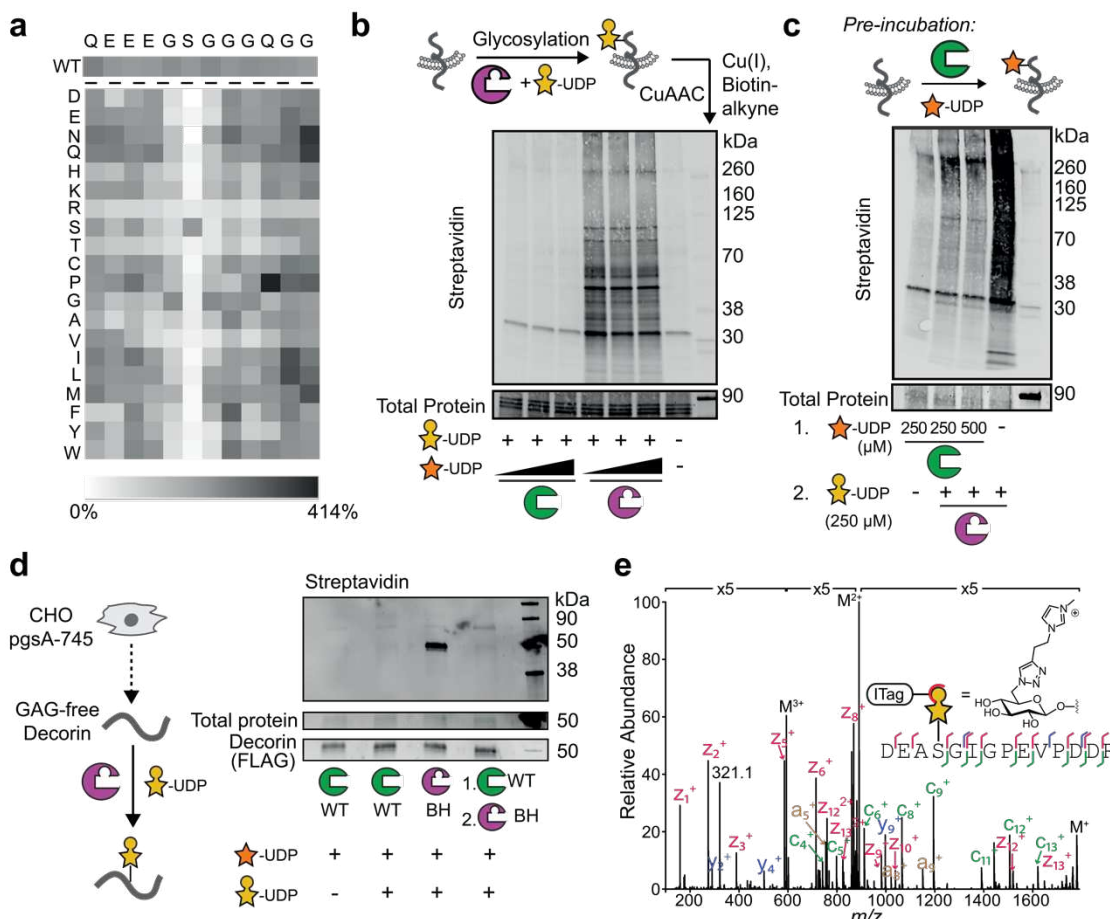
11  
12 The biosynthesis of HS and CS commences via a common O-linked glycan “linker”  
13 modification consisting of a glucuronic acid (GlcA), two galactoses (Gal) and a xylose (Xyl) in  
14 the GlcA(β-3)Gal(β-3)Gal(β-4)Xyl(β-)Ser sequence (Fig. 1a), with optional modifications  
15 such as phosphorylation on the core Xyl.<sup>7,24</sup> The first glycosylation step attaching Xyl to Ser  
16 is subject to biosynthetic redundancy by the xylosyltransferase isoenzymes XT1 and XT2  
17 that utilize uridine diphosphate (UDP)-Xyl as a substrate. The isoenzymes share 60% amino  
18 acid identity but display tissue-specific expression patterns and dysfunctions are associated  
19 with different genetic disorders - Desbuquois Dysplasia type 2 and Spondylo-Ocular  
20 Syndrome for patient *XYLT1* and *XYLT2* mutations, respectively.<sup>25-28</sup> Differential roles in  
21 physiology have been attributed to XT1 and XT2.<sup>29,30</sup> Although XT2 appears to be the  
22 dominant isoenzyme in cell lines and serum,<sup>31,32</sup> *Xylt1* and *Xylt2* knockout (KO) mice display

1 differential defects in development.<sup>29,30</sup> Despite their importance in physiology and the  
2 unanswered questions about substrate repertoires, it is not possible to directly profile the  
3 substrate proteins or even individual glycosylation sites of XT isoenzymes.  
4  
5 Here, we employ a chemical biology tactic termed bump-and-hole (BH) engineering to probe  
6 the substrates of human xylosyltransferases in living cells. Based on structural  
7 considerations, we mutate a bulky amino acid in the active site of XT1 to a smaller residue to  
8 accept a chemically modified UDP-sugar that is not accepted by the wildtype (WT) enzyme.  
9 The chemical modification contains an azide group for bioorthogonal incorporation of  
10 fluorophores or biotin (Fig. 1a). After in-depth biochemical characterisation, we install the  
11 XT1 BH system in mammalian cells to directly visualise and probe proteoglycans. Using MS  
12 glycoproteomics, we find confirm that BH-engineered XT1 modifies the native glycosylation  
13 site of a model proteoglycan in living mammalian cells. We further show that BH engineering  
14 can be applied to the isoenzyme XT2, allowing differential glycoproteomics in future  
15 applications. By developing an XT BH system, we simultaneously gain the ability to find new  
16 proteoglycans and define the protein substrate specificities of XT isoenzymes.  
17

## 18 **Results**

20 **Design of a xylosyltransferase bump-and-hole system**  
21 Our XT BH design was prompted by biosynthetic and structural considerations (Fig. 1b). In  
22 the absence of an acetamide group that has featured in numerous tool development  
23 approaches of other sugars,<sup>33,34</sup> the most common approach to develop bioorthogonal  
24 reporters of monosaccharides is the replacement of hydroxyl with azido groups.<sup>35-37</sup> Beahm  
25 et al. developed a 4-azido-substituted Xyl analogue that is incorporated into proteoglycans  
26 by XT1,<sup>38</sup> but the corresponding UDP-sugar could not be biosynthesized in mammalian cells  
27 since there is no salvage pathway for Xyl.<sup>39</sup> The bump-and-hole tactic uses substrate  
28 analogues that would normally not be accepted by GTs.<sup>40-42</sup> We sought to employ this  
29 feature to our benefit and reprogram XTs to accept a UDP-sugar that is not accepted by WT-  
30 XT1 but can be biosynthesized in mammalian cells. WT-XT1 has been reported to use UDP-  
31 6AzGlc with approx. 20-fold lower enzymatic efficiency than UDP-Xyl.<sup>43</sup> We opted to develop  
32 a mutant with reversed selectivity to accept UDP-6AzGlc over UDP-Xyl. We recently  
33 reported the crystal structure of XT1, revealing a two-lobe architecture.<sup>16</sup> Since XT1 contains  
34 an unusually constricted UDP-Xyl binding site that prevents the use of larger UDP-sugars  
35 such as UDP-6AzGlc, we deemed it possible to generate additional space (a “hole”) in the  
36 active site by mutation. We identified several bulky “gatekeeper” amino acids in close

1 proximity to C-5 of UDP-Xyl, namely Trp392, Leu525 and Leu526 (Fig. 1b). We designed,  
 2 expressed and purified from Expi293 cells a total of 16 XT1 single and double mutants in



3  
 4 **Fig. 2: BH engineering preserves protein substrate specificity of XT1.** **a**, *in vitro* glycosylation of a  
 5 peptide substrate panel based on the bikunin peptide indicated at the top of the panel as assessed by  
 6 a luminescence assay, with every position substituted for each of the 20 amino acids. Intensity of grey  
 7 scale indicates % turnover. The WT bikunin peptide was present 12 times in the panel (copied in the  
 8 top row) and all other peptide reactions were normalised on the average of these 12 data points. Data  
 9 are from one out of three independent experiments. **b**, *in vitro* glycosylation of a membrane protein  
 10 fraction of XT2-KO CHO<sup>KO Xyl2t</sup> cells as assessed by streptavidin blot. Reactions contained 250 μM  
 11 UDP-6AzGlc and 100, 200 or 300 μM UDP-Xyl, respectively, and were reacted with biotin-alkyne  
 12 before blotting. Data are from one out of two independent experiments. **c**, glycosylation by BH-  
 13 XT1/UDP-6AzGlc can be prevented by pre-incubation with WT-XT1/UDP-Xyl. Reactions were  
 14 processed as in **b**. Data are from one experiment. **d**, *in vitro* glycosylation of a GAG-free preparation  
 15 of human decorin purified from pgA-745 CHO cells as assessed by streptavidin blot. Reactions were  
 16 run with 250 μM UDP-sugars and processed as in **b** and **c**. Data are from one out of two independent  
 17 experiments. **e**, analysis of the glycosylation site on decorin introduced by BH-XT1 by mass  
 18 spectrometry and ETD fragmentation. Decorin was *in vitro* glycosylated as in **c**, subjected to CuAAC  
 19 with ITAG-azide,<sup>44</sup> digested and subjected to MS-glycoproteomics. Fragments are annotated on the  
 20 tryptic peptide from mature decorin. 321.1 denotes a signature ion from chemically modified sugar.  
 21 Data are from one experiment.

1 which these residues were replaced with smaller amino acids (Fig. 1c, Supporting Fig. 1).  
2 We assessed *in vitro* glycosylation of a well-known bikunin substrate peptide in an HPLC-  
3 based assay to assess glycosylation from the sugar donors UDP-Xyl, UDP-6AzGlc and, as a  
4 substrate of intermediate size of the “bump”, UDP-glucose.<sup>16</sup>

5

6 WT-XT1 displayed exclusive activity for UDP-Xyl in our hands, in contrast to recently  
7 reported residual use of UDP-6AzGlc.<sup>43</sup> Most mutants displayed either no activity at all or  
8 were still selective for UDP-Xyl, with some displaying low activity toward UDP-Glc. Strikingly,  
9 the mutant Leu526Gly preferred UDP-6AzGlc as a substrate, with 7-8-fold higher turnover  
10 than using UDP-Xyl or UDP-Glc in an endpoint assay. Compared to the Leu526Gly mutant  
11 (henceforth termed “BH-XT1”), the construct Leu526Ala displayed no such selectivity, with  
12 equal activity on all three UDP-sugars (Fig. 1c). These data highlight the need for a detailed  
13 structure-function investigation in the design of bump-and-hole mutants. We next determined  
14 the kinetic constants for the native and BH enzyme-substrate pairs (Fig. 1d, Supporting Figs  
15 2, 3). We found that the  $K_m$  of the BH pair was conserved compared to the WT pair, while the  
16  $k_{cat}$  was reduced threefold. In contrast, BH-XT1 uses UDP-Xyl with an approx. 10-fold lower  
17 catalytic efficiency than UDP-6AzGlc, indicating that the native substrate UDP-Xyl might not  
18 be able to outcompete UDP-6AzGlc in cells. Taken together, we established a sensitive  
19 structure-activity relationship in the development of a suitable XT1 bump-and-hole mutant.  
20 BH-XT1 fulfilled the crucial pre-requisite of preferring a chemically modified substrate that is  
21 not used by the WT enzyme.

22

### 23 **Bump-and-hole engineering retains the peptide specificity of WT-XT1**

24 To assess whether BH engineering retains the peptide substrate preference of WT-XT1, we  
25 tested the bump-and-hole enzyme-substrate pair (BH-XT1, UDP-6AzGlc) with a panel of 240  
26 substrate peptides in an *in vitro* glycosylation assay. The panel contained derivatives of the  
27 well-characterised bikunin XT1 substrate peptide in which each amino acid was substituted  
28 with each of the 20 proteinogenic amino acids. We had previously used the same peptide  
29 panel to extract peptide substrate preferences of the native enzyme-substrate pair (WT-XT1,  
30 UDP-Xyl) in a luminescence-based assay.<sup>16</sup> We found that the peptide substrate preferences  
31 were remarkably conserved between WT- and BH-XT1 (Fig. 2a, for WT peptide preference  
32 see Briggs and Hohenester<sup>16</sup>). For instance, introducing basic Lys or Arg residues anywhere  
33 in the substrate peptide lowered enzyme activity, while acidic Glu and Asp tended to  
34 increase activity. A notable data point was the swap of Glu at -4 position to Asp which led to  
35 a decrease in turnover for both WT- and BH-XT1.<sup>16</sup> As in WT-XT1, substitutions of glycine  
36 residues at positions -1 and +1 of the central Ser were not well-tolerated by BH-XT1. An

1 exception was substitution of Gly at +1 position to hydrophobic amino acids Leu, Met or Phe,  
2 which led to residual activity in BH- but not WT-XT1. Since this Gly is in contact with Leu526  
3 in WT-XT1, we reasoned that the Leu526Gly “hole” left space for substitutions to larger  
4 hydrophobic amino acids in substrate peptides. Since these were the only reproducible  
5 differences between WT and BH-XT1 (other replicates in Supporting Fig. 4) and relatively  
6 low in number in a 240-member peptide library, we concluded that BH engineering exhibits  
7 conservation of peptide substrate preference *in vitro*.

8

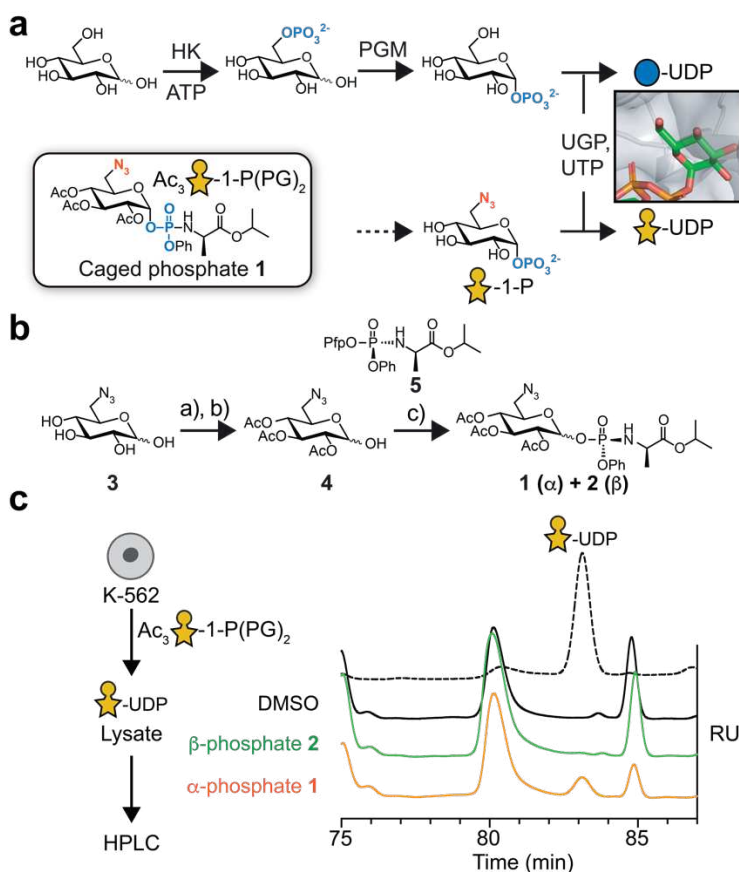
### 9 **BH-XT1 glycosylates proteoglycans at GAG attachment sites *in vitro***

10 We next assessed whether BH-XT1 retains the activity of WT-XT1 to prime GAG attachment  
11 sites on proteoglycan backbones. We prepared membrane fractions from Chinese Hamster  
12 Ovary (CHO) cells with or without KO for endogenous xylosyltransferase genes *Xylt1* and  
13 *Xylt2*.<sup>10</sup> Membrane fractions were incubated with recombinant WT- or BH-XT1 as well as  
14 synthetic UDP-Xyl and UDP-6AzGlc, followed by reaction with alkyne-biotin under copper-  
15 catalysed azide-alkyne cycloaddition (CuAAC) “click” conditions. Analysis by streptavidin blot  
16 suggested labelling of lysate proteins with 6AzGlc only when BH-XT1, but not WT-XT1 was  
17 present (Supporting Fig. 5). Since *Xylt2* is the major xylosyltransferase gene expressed in  
18 CHO cells,<sup>10</sup> we used CHO<sup>KO Xylt2</sup> cells for further *in vitro* glycosylation experiments. We  
19 established that labelling by BH-XT1 with UDP-6AzGlc could not be outcompeted with  
20 increasing concentrations of UDP-Xyl, suggesting that BH-XT1 specifically and potently  
21 recognises UDP-6AzGlc as a substrate (Fig. 2b). Pre-incubation of the membrane protein  
22 fraction with WT-XT1 and UDP-Xyl abrogated incorporation of 6AzGlc by BH-XT1,  
23 suggesting that the same glycosylation sites are introduced by both enzymes (Fig. 2c).

24 We next confirmed *in vitro* that BH-XT1 emulates the activity of WT-XT1 to glycosylate  
25 proteoglycans. Human decorin has a single site of GAG attachment. Recombinant  
26 expression in the CHO cell mutant pgsA-745 that lacks endogenous XT activity results in a  
27 GAG-free decorin preparation.<sup>7,8</sup> We incubated this GAG-free decorin with either WT- or BH-  
28 XT1 in the presence of UDP-Xyl and/or UDP-6AzGlc, followed by CuAAC with alkyne-biotin  
29 and streptavidin blot. (Fig. 2d). While WT-XT1 activity did not lead to discernible streptavidin  
30 signal on decorin, BH-XT1 in the presence of UDP-6-AzGlc led to intense streptavidin signal  
31 that could be abrogated by pre-incubation of decorin with WT-XT1 and UDP-Xyl. These data  
32 indicate that the single GAG attachment site was blocked with a xylose residue by WT-XT1,  
33 preventing BH-XT1 activity. We observed the same behaviour in GAG-free preparation of  
34 human glypcan 1 (Supporting Fig. 6), suggesting that BH-XT1 recapitulates the activity of  
35 WT-XT1 across a range of proteoglycans.

36 We confirmed the glycosylation site modified by BH-XT1 on decorin by tandem mass  
37 spectrometry (MS). Two fragmentation methods are routinely employed for O-glycopeptides.

1 High energy collision-induced dissociation (HCD) primarily fragments the glycosidic bond to  
2 detect glycan oxonium ions while electron transfer dissociation (ETD) fragments the peptide  
3 backbone to allow glycan site annotation. The clickable azide tag was essential to improve  
4 sugar identification in mass spectra, allowing incorporation of functional groups that are  
5 beneficial to analysis. Specifically, we employed a clickable imidazolium tag (ITag) that  
6 carries a permanent positive charge and increased the charge state of glycopeptides,  
7 allowing direct glycosylation site annotation.<sup>44</sup> We used HCD first to fragment decorin-  
8 derived (glyco-)peptides (Supporting Fig. 7a) and upon detection of an ITag-containing,  
9 6AzGlc-derived signature ion, triggered ETD on the same glycopeptide.<sup>34,40,42,44</sup>

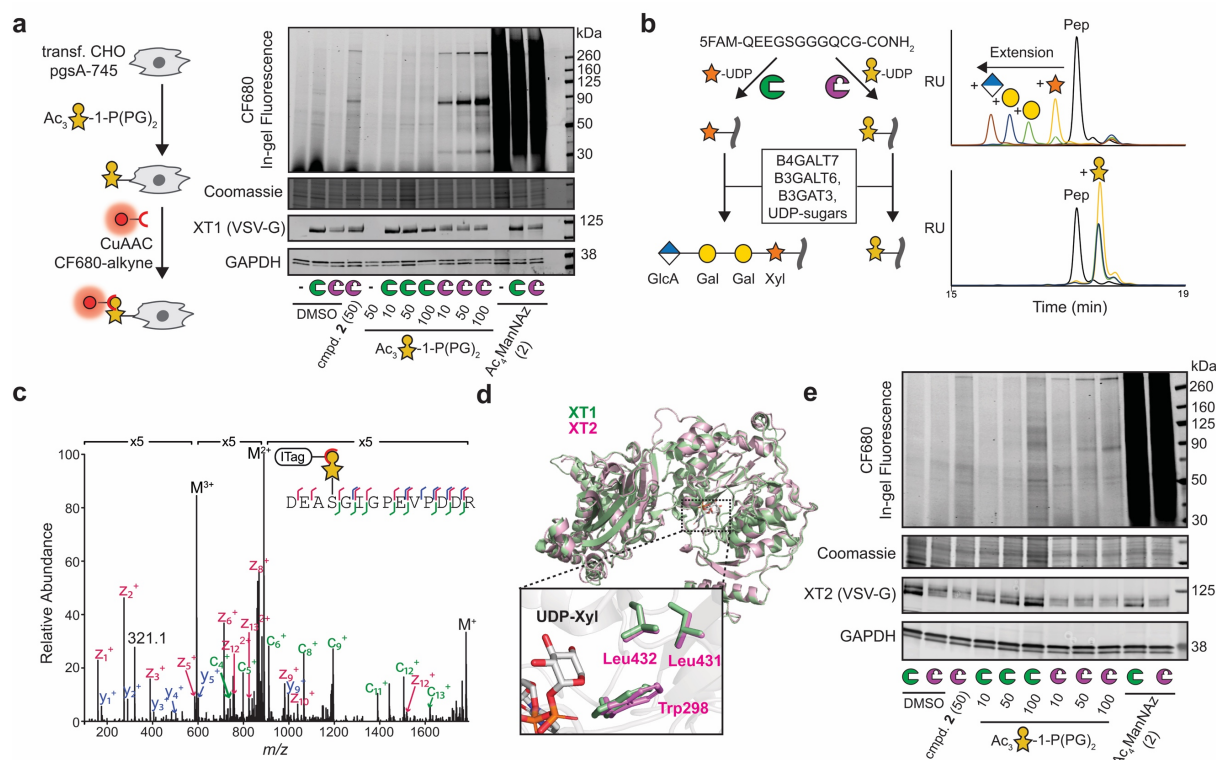


10  
 11 **Fig. 3:** Biosynthesis of UDP-6AzGlc. **a**, biosynthetic pathway of UDP-Glc via hexokinase (HK),  
 12 phosphoglucomutase (PGM) and UDP-Glc pyrophosphorylase (UGP). Biosynthesis of UDP-6AzGlc  
 13 from caged phosphate **1** bypasses the HK and PGM steps. Insert: crystal structure of UGP with UDP-  
 14 Glc indicating that the 6-OH group protrudes into an open cavity (PDB 4R7P). **b**, synthesis of caged  
 15 sugar-1-phosphates **1** and **2** from 6AzGlc **3**. **c**, biosynthesis of UDP-6AzGlc in K562 cells as  
 16 assessed by ion exchange HPLC of lysates fed with compounds **1** or **2**. Data are from one out of two  
 17 independent experiments. Reagents and conditions: a) Ac<sub>2</sub>O, pyridine, DMAP, r.t., 90%; b) AcOH,  
 18 ethylene diamine, r.t. 45-73%; c) 2 M LDA in THF, **5**, -78°C to -70°C, **(1)** 60% **(2)** 9.8%. DMAP = 4-  
 19 Dimethylaminopyridine; LDA = lithium diisopropylamide. RU = relative units.

1 Decorin is proteolytically processed during secretion to remove a propeptide and shorten the  
2 N-terminus.<sup>45</sup> ETD allowed for direct identification of Ser34 as the attachment site of 6AzGlc  
3 by BH-XT1 on this mature form, consistent with Ser34 being the site of cellular GAG  
4 attachment (Fig. 2e).<sup>46</sup> Taken together, these results suggest that the XT1 bump-and-hole  
5 enzyme-substrate pair glycosylates native GAG attachment sites in proteoglycans *in vitro*.  
6

7 **Development of a cellular XT1 bump-and-hole system**

8 Application of a GT BH system in living cells requires biosynthesis of the nucleotide-sugar. In  
9 general, caged, membrane-permeable monosaccharide precursors are employed with ester  
10 modifications that are deprotected in the cytosol. Free monosaccharides can then be  
11 converted to UDP-sugars before transport to the Golgi.<sup>41,42,47</sup> Although human cells are  
12 devoid of a salvage pathway for UDP-Xyl, our strategic use of UDP-6AzGlc provided an  
13 opportunity for cellular application by hijacking the biosynthetic pathway for UDP-Glc  
14 instead. Glc is activated in mammalian cells first by phosphorylation to Glc-6-phosphate and,  
15 subsequently, isomerization by phosphoglucomutase PGM to Glc-1-phosphate (Fig. 3a).  
16 Conversion to UDP-Glc then features the enzymes UDP-Glc pyrophosphorylase 1 or 2,  
17 UGP1/2. Since phosphorylation at the 6-position was prevented by the presence of an azido  
18 group, we sought to bypass the kinase and PGM steps and provide a sugar-1-phosphate as  
19 a direct substrate for UGP1/2. We were encouraged by analysis of the UGP1/UDP-Glc co-  
20 crystal structure where the UDP-Glc 6-hydroxyl group is solvent-exposed, suggesting that an  
21 azido group at that position should be tolerated by the enzyme (Fig. 3a).<sup>48</sup> While we and  
22 others have made sugar-1-phosphates caged as labile bis-S-acetylthioethyl (SATE)  
23 phosphotriesters, synthesis of SATE-caged 6AzGlc-1-phosphate failed in our hands.<sup>42,49,50</sup>  
24 Instead, we took inspiration from the increasingly popular protide technology that has gained  
25 attention to cage phosphates in antiviral nucleotides.<sup>51,52</sup> To our knowledge, such chemistry  
26 has not been applied to sugar-1-phosphates yet, but for instance to sugar-6-phosphates.<sup>53,54</sup>  
27 We synthesized phosphoamidate diester **1** to be deprotected by esterases in the cytosol  
28 (Fig. 3a).<sup>51</sup> The synthesis proceeded from lactol mixture **3** via the intermediate triacetate **4**.  
29 Treatment of **4** with **5** under basic conditions yielded both  $\alpha$ -phosphate **1** (60% yield) and  $\beta$ -  
30 phosphate **2** (9.8% yield) (Fig. 3b).<sup>55</sup> Since UGP1/2 is naturally restricted to  $\alpha$ -configured  
31 Glc-1-phosphate,  $\beta$ -phosphate **2** served as a negative control in feeding experiments.  
32 Feeding K-562 cells the  $\alpha$ -phosphate **1** led to notable and reproducible biosynthesis of UDP-  
33 6AzGlc (Fig. 3c). In turn,  $\beta$ -configured **2** led to negligible UDP-6AzGlc levels. These data  
34 suggest that  $\alpha$ -phosphate **1** is a suitable precursor to deliver UDP-6AzGlc to mammalian  
35 cells by entering the UDP-Glc biosynthetic pathway.  
36



1  
2 **Fig. 4: BH-engineered xylosyltransferases label proteoglycans in mammalian cells. a,** chemical  
3 tagging of proteoglycans on pgsA-745 CHO cells as assessed by in-gel fluorescence. Cells stably  
4 expressing WT- or BH-XT1 or non-transfected were fed with compounds in the indicated  
5 concentrations in  $\mu$ M before on-cell CuAAC. Data are from one out of two independent replicates. **b,**  
6 6AzGlc is not elongated by GAG linker enzymes. Fluorescently labelled bikunin-derived peptide was  
7 incubated with WT-XT1/UDP-Xyl or BH-XT1/UDP-6AzGlc and subsequently with the indicated soluble  
8 glycosyltransferases<sup>7</sup> and corresponding UDP-sugars. Elongation was assessed on each step by  
9 HPLC. Data are from one experiment each with different combinations of transferases. **c,** analysis of  
10 the glycosylation site on decorin introduced by BH-XT1 in living cells by mass spectrometry and ETD  
11 fragmentation. Decorin was co-expressed with BH-XT1 in cells fed with **1**, then subjected to CuAAC  
12 with ITag-azide,<sup>44</sup> digested and subjected to MS-glycoproteomics. Fragments are annotated on the  
13 tryptic peptide from mature decorin. Not all fragments are shown. 321.1 denotes a signature ion from  
14 chemically modified sugar. Data are from one experiment. **d,** structural alignment between the crystal  
15 structure of human XT1 (PDB 6EJ7, green) and the AlphaFold structure of human XT2 (accession no.  
16 Q9H1B5, purple) with aligned gatekeeper residues in the insert. **e,** BH-XT2 chemically tags  
17 proteoglycans on mammalian cells. Cells stably transfected with WT- or BH-XT2 were fed and treated  
18 as in **a**. Data are from one out of two independent experiments.

19  
20 In accordance with biosynthetic experiments, the  $\beta$ -configured 6AzGlc-1-phosphate **2**  
21 yielded a weak and diffuse labelling signal, indicating that UDP-6AzGlc biosynthesis is a  
22 direct prerequisite for cellular chemical tagging of glycoproteins by BH-XT1.

23

1 We next employed UDP-6AzGlc delivery to establish a cellular XT1 bump-and-hole system.  
2 Stable transfection of pgsA-745 CHO cells with WT- or BH-XT1 was followed by feeding the  
3 6AzGlc-1-phosphate precursor **1**. After overnight incubation, a CuAAC reaction was  
4 performed to attach clickable alkyne-CF680 on the cell surface while keeping cells  
5 alive.<sup>34,42,47</sup> Surplus click reagents were washed away, cells lysed and fluorophore  
6 incorporation assessed by SDS-PAGE and in-gel fluorescence (Fig. 4a). Minimal  
7 background fluorescence was observed in cells fed with DMSO or only expressing WT-XT1,  
8 even when fed with increasing concentrations of 6AzGlc-1-phosphate precursor **1**. In the  
9 presence of BH-XT1, clear fluorescent proteins were observed at 38 kDa, 90 kA and 260  
10 kDa. With increasing feeding concentration of **1**, a dose-dependent increase of fluorescence  
11 was observed, along with labelled protein bands of lower intensity, especially at 50 kDa.  
12

### 13 **XT bump-and-hole engineering identifies proteoglycans in mammalian cells**

14 Xylosyltransferase BH engineering is poised to allow the identification of new proteoglycans,  
15 a feat that normally requires elaborate methods of glycopeptide enrichment and  
16 characterisation.<sup>9,20,22</sup> To establish an MS-glycoproteomics workflow, it was important to  
17 assess whether 6AzGlc, like Xyl, was extended to a functional GAG linker tetrasaccharide.  
18 We recently reported an enzymatic method for extension of xylosylated glycopeptides by  
19 recombinant preparations of the glycosyltransferases B4GALT7, B3GALT6 and B3GAT3  
20 (termed linker enzymes) in the presence of UDP-galactose (UDP-Gal) and UDP-glucuronic  
21 acid (UDP-GlcA). Employing a fluorescently labelled bikunin-derived peptide, we first  
22 confirmed by HPLC that the linker enzymes extend a Xyl moiety introduced by WT-XT1 to  
23 the full tetrasaccharide. In contrast, a 6AzGlc-modified peptide did not shift in retention time  
24 upon incubation with the GTs and UDP-sugars (Fig. 4b). We concluded that 6AzGlc is a  
25 chain-terminating modification that is not extended to functional GAG chains. We interpreted  
26 this feature is an advantage for the discovery of proteoglycans by MS due to the  
27 substantially decreased complexity of the modification that is convenient to analyse. To this  
28 end, we next performed an MS-glycoproteomics experiment to identify the glycosylation site  
29 of a model proteoglycan in living cells. FLAG-tagged human decorin was overexpressed in  
30 pgsA-745 CHO cells that expressed BH-XT1 and were fed with 6AzGlc-1-phosphate  
31 precursor **1**. Following immunoprecipitation, decorin was subjected to a CuAAC reaction with  
32 an iTag-azide, digested and subjected to mass spectrometry by HCD-triggered ETD  
33 fragmentation. We confirmed unambiguously that Ser34 was glycosylated by BH-XT1 inside  
34 mammalian cells, confirming the bump-and-hole approach as suitable to identify  
35 proteoglycans including native Xyl attachment sites (Supporting Fig. 7b, Fig. 4c).  
36

1 It is currently not known why the mammalian genome encodes two xylosyltransferase  
2 isoenzymes. To distinguish their protein substrate profiles, we extended the BH method from  
3 XT1 to the second isoenzyme xylosyltransferase 2. A structural overlay between the XT1  
4 crystal structure and the XT2 AlphaFold2 structure highlighted conservation of amino acids  
5 interacting with UDP-Xyl (Fig. 4d). In parallel to XT1, we cloned the BH-XT2 mutant L432G  
6 and stably transfected pgsA-745 CHO cells with either WT- or BH-XT2. Feeding with  
7 6AzGlc-1-phosphate precursor **1** and cell-surface CuAAC reaction indicated that BH-XT2  
8 labels a similar protein repertoire as BH-XT1 but at lower intensity (Fig. 4e).

9

## 10 Discussion

11 The importance of proteoglycans in physiology is undisputed, as the vast majority of  
12 signalling events between cells or with the extracellular matrix are modulated by the  
13 associated GAG chains. While great efforts are being made to understand the details of  
14 GAG polysaccharide sequence on biology,<sup>10,14,21,56,57</sup> we still lack important information on  
15 the first step of glycosylation to the protein backbone. The two human xylosyltransferases  
16 display limited tissue selectivity and differences in attached GAG sequences but we still lack  
17 fundamental detail on their individual biological functions.<sup>27,30-32,58</sup> Furthermore, only a  
18 relatively small number of annotated mammalian proteoglycans has been mapped, with new  
19 annotations requiring considerable effort.<sup>9</sup> A chemical tool to dissect XT1/2 biology must  
20 accurately report on XT1/2 activity while being orthogonal to other glycosylation events in the  
21 secretory pathway and deliverable to living mammalian cells. The use of a UDP-Glc  
22 analogue matched these pre-requisites. Both catalytic efficiency and peptide substrate  
23 preference of the XT1 bump-and-hole enzyme-substrate pair were remarkably conserved,  
24 which we attribute to the careful structure-based design of the pair. Labelling signal was  
25 dependent on the presence of BH-XT1, indicating that 6AzGlc does not enter other major  
26 glycosylation pathways. The finding that 6AzGlc is not extended to the common GAG linker  
27 tetrasaccharide was an advantage for mass spectrometry since the sugar is structurally well-  
28 defined and did not require any glycosidase treatment steps prior to analysis. Annotation  
29 was further simplified by the availability of the iTag technology to facilitate mass  
30 spectrometry. Furthermore, a chain-terminating, clickable inhibitor of chain extension has the  
31 potential to be employed to study GAG biology *in vitro* or *in vivo*,<sup>38,59,60</sup> substantially  
32 expanding our toolbox.

33 Establishing a cellular XT bump-and-hole system required a biosynthetic entry point for  
34 UDP-6AzGlc. Previously used per-acetylated 6AzGlc was not a suitable precursor for  
35 glycosylation in our hands,<sup>35</sup> but we note that cell lines from different organisms can vary in  
36 their biosynthetic potential.<sup>61</sup> Nevertheless, a protide-based caged sugar-1-phosphate was a  
37 reliable precursor for UDP-6AzGlc to fashion a cellular bump-and-hole system. We did not

1 assess whether UDP-6AzGlc was used by other glycosyltransferases, but cell surface  
2 labelling experiments suggested that BH-XT activity was necessary to introduce the  
3 chemical modification into glycoproteins.  
4 While XT2 appears to be the dominant isoenzyme expressed in humans, dysfunctions in  
5 both enzymes lead to severe yet differential disorders in mouse models and in patients.<sup>29-32</sup>  
6 After fully characterising an XT1 BH system, we designed a functional BH-XT2 mutant  
7 simply based on structural homology, showcasing the reliability of the tactic as well as the  
8 importance of structural data. Our work will establish the fine differences between XT1 and  
9 XT2 and identify proteoglycans in a range of different model systems.

10

## 11 **Acknowledgements**

12 We thank Ganka Bineva-Todd and Andrea Marchesi for help with chemical synthesis and  
13 analysis, and Khadija Babiker for help with cloning similar constructs. We thank Chloë  
14 Roustan, Svend Kjaer and the Francis Crick Institute Structural Biology Science Technology  
15 Platform for help with protein expression and purification. We further thank Tania  
16 Auchynnikava and Mark Skehel for help with mass spectrometry, and the Crick Proteomics,  
17 Chemical Biology and Cell Services Science Technology Platforms for valuable support. This  
18 work was supported by the Francis Crick Institute (to B. S.) which receives its core funding  
19 from Cancer Research UK (CC2127, CC2068), the UK Medical Research Council (CC2127,  
20 CC2068) and Wellcome Trust (CC2127, CC2068), the BBSRC (BB/T01279X/1 to E. H. and  
21 B. S., BB/V008439/1 to B. S.), the EPSRC (EP/T007397/1 to G.J.M) and the MRC  
22 (MR/T019522/1 to G.J.M). We also thank the EPSRC UK National Mass Spectrometry  
23 Facility (NMSF) at Swansea University. This work was supported by the Novo Nordisk  
24 Foundation grant No. NNF22OC0073736 (to R. L. M.). L. I. W. gratefully acknowledges  
25 funding from the European Research Council (ERC) under the European Union's Horizon  
26 2020 research and innovation programme (Grant agreement No 851448). For the purpose of  
27 Open Access, the author has applied a CC BY public copyright licence to any Author  
28 Accepted Manuscript version arising from this submission.

29

30

## 31 **References**

- 32 1. Xu, D. & Esko, J. D. Demystifying Heparan Sulfate–Protein Interactions. *Annu Rev Biochem* **83**, 129–157 (2014).
- 33 2. Bishop, J. R., Schuksz, M. & Esko, J. D. Heparan sulphate proteoglycans fine-tune  
34 mammalian physiology. *Nature* **446**, 1030–1037 (2007).
- 35 3. Pickford, C. E. *et al.* Specific Glycosaminoglycans Modulate Neural Specification of  
36 Mouse Embryonic Stem Cells. *Stem Cells* **29**, 629–640 (2011).
- 37 4. Kreuger, J. *et al.* Fibroblast growth factors share binding sites in heparan sulphate.  
38 *Biochem J* **389**, 145–150 (2005).

1 5. Mizumoto, S. & Yamada, S. Congenital Disorders of Deficiency in Glycosaminoglycan  
2 Biosynthesis. *Front Genet* **12**, 717535 (2021).

3 6. Zhang, L. & Esko, J. D. Amino acid determinants that drive heparan sulfate assembly  
4 in a proteoglycan. *J of Biol Chem* **269**, 19295–19299 (1994).

5 7. Sammon, D. *et al.* Molecular mechanism of decision-making in glycosaminoglycan  
6 biosynthesis. *Nat Commun* **2023** **14**, 1–13 (2023).

7 8. Esko, J. D., Stewart, T. E. & Taylor, W. H. Animal cell mutants defective in  
8 glycosaminoglycan biosynthesis. *Proc Natl Acad Sci U S A* **82**, 3197–3201 (1985).

9 9. Zhang, P. *et al.* Heparan Sulfate Organizes Neuronal Synapses through Neurexin  
10 Partnerships. *Cell* **174**, 1450–1464.e23 (2018).

11 10. Chen, Y. H. *et al.* The GAGOme: a cell-based library of displayed  
12 glycosaminoglycans. *Nat Methods* **15**, 881–888 (2018).

13 11. Qiu, H. *et al.* A mutant-cell library for systematic analysis of heparan sulfate structure–  
14 function relationships. *Nat Methods* **2018** **15**, 889–899 (2018).

15 12. Ji, S. K. *et al.* PTP $\sigma$  functions as a presynaptic receptor for the glypican-4/LRRTM4  
16 complex and is essential for excitatory synaptic transmission. *Proc Natl Acad Sci U S*  
17 **A** **112**, 1874–1879 (2015).

18 13. Kamimura, K. *et al.* Perlecan regulates bidirectional Wnt signaling at the Drosophila  
19 neuromuscular junction. *J Cell Biol* **200**, 219–233 (2013).

20 14. Merry, C. L. R., Lindahl, U., Couchman, J. & Esko, J. D. Proteoglycans and Sulfated  
21 Glycosaminoglycans. *Essentials of Glycobiology* (2022)

22 15. Noborn, F. & Sterky, F. H. Role of neurexin heparan sulfate in the molecular assembly  
23 of synapses – expanding the neurexin code? *FEBS J* **290**, 252–265 (2023).

24 16. Briggs, D. C. & Hohenester, E. Structural Basis for the Initiation of Glycosaminoglycan  
25 Biosynthesis by Human Xylosyltransferase 1. *Structure* **26**, 801–809.e3 (2018).

26 17. Zhang, L., David, G. & Esko, J. D. Repetitive Ser-Gly Sequences Enhance Heparan  
27 Sulfate Assembly in Proteoglycans. *J Biol Chem* **270**, 27127–27135 (1995).

28 18. Ramarajan, M. G. *et al.* Mass spectrometric analysis of chondroitin sulfate-linked  
29 peptides. *J Protein Proteomics* **2022** **13**, 187–203 (2022).

30 19. Ly, M., Laremore, T. N. & Linhardt, R. J. Proteoglycomics: Recent progress and future  
31 challenges. *OMICS* **14**, 389–399 (2010).

32 20. Noborn, F., Nilsson, J. & Larson, G. Site-specific glycosylation of proteoglycans: A  
33 revisited frontier in proteoglycan research. *Matrix Biology* vol. 111 289–306 (2022).

34 21. Persson, A., Nikpour, M., Vorontsov, E., Nilsson, J. & Larson, G. Domain Mapping of  
35 Chondroitin/Dermatan Sulfate Glycosaminoglycans Enables Structural  
36 Characterization of Proteoglycans. *Mol Cell Proteom* **20**, 100074 (2021).

37 22. Noborn, F. *et al.* A Glycoproteomic Approach to Identify Novel Proteoglycans. *Meth  
38 Mol Biol* **2303**, 71–85 (2022).

39 23. Noborn, F. *et al.* Site-specific identification of heparan and chondroitin sulfate  
40 glycosaminoglycans in hybrid proteoglycans. *Sci Rep* **6**, 1–11 (2016).

41 24. Wen, J. *et al.* Xylose phosphorylation functions as a molecular switch to regulate  
42 proteoglycan biosynthesis. *Proc Natl Acad Sci U S A* **111**, 15723–15728 (2014).

43 25. Bui, C. *et al.* XYLT1 mutations in desbuquois dysplasia type 2. *Am J Hum Genet* **94**,  
44 405–414 (2014).

45 26. Munns, C. F. *et al.* Homozygosity for frameshift mutations in XYLT2 result in a  
46 spondylo-ocular syndrome with bone fragility, cataracts, and hearing defects. *Am J  
47 Hum Genet* **96**, 971–978 (2015).

48 27. Wilson, I. B. H. The never-ending story of peptide O-xylosyltransferase. *Cell Mol Life  
49 Sci* **61**, 794–809 (2004).

50 28. Götting, C., Kuhn, J., Zahn, R., Brinkmann, T. & Kleesiek, K. Molecular cloning and  
51 expression of human UDP-D-xylose: Proteoglycan core protein  $\beta$ -D-xylosyltransferase  
52 and its first isoform XT-II. *J Mol Biol* **304**, 517–528 (2000).

53 29. Ferencz, B. *et al.* Xylosyltransferase 2 deficiency and organ homeostasis. *Glycoconj J*  
54 **37**, 755 (2020).

1 30. Taieb, M., Ghannoum, D., Barré, L. & Ouzzine, M. Xylosyltransferase I mediates the  
2 synthesis of proteoglycans with long glycosaminoglycan chains and controls  
3 chondrocyte hypertrophy and collagen fibers organization in the growth plate. *Cell*  
4 *Death Dis* 2023 **14**: 1–13 (2023).

5 31. Roch, C., Kuhn, J., Kleesiek, K. & Götting, C. Differences in gene expression of  
6 human xylosyltransferases and determination of acceptor specificities for various  
7 proteoglycans. *Biochem Biophys Res Commun* **391**, 685–691 (2010).

8 32. Kuhn, J. *et al.* Xylosyltransferase II is the predominant isoenzyme which is  
9 responsible for the steady-state level of xylosyltransferase activity in human serum.  
10 *Biochem Biophys Res Commun* **459**, 469–474 (2015).

11 33. Choi, J. *et al.* Engineering Orthogonal Polypeptide GalNAc-Transferase and UDP-  
12 Sugar Pairs. *J Am Chem Soc* **141**, 13442–13453 (2019).

13 34. Debets, M. F. *et al.* Metabolic precision labeling enables selective probing of O-linked  
14 N-acetylgalactosamine glycosylation. *Proc Natl Acad Sci U S A* **117**, 25293–25301  
15 (2020).

16 35. Darabedian, N., Gao, J., Chuh, K. N., Woo, C. M. & Pratt, M. R. The Metabolic  
17 Chemical Reporter 6-Azido-6-deoxy-glucose Further Reveals the Substrate  
18 Promiscuity of O-GlcNAc Transferase and Catalyzes the Discovery of Intracellular  
19 Protein Modification by O-Glucose. *J Am Chem Soc* **140**, 7092–7100 (2018).

20 36. Darabedian, N. *et al.* O-Acetylated Chemical Reporters of Glycosylation Can Display  
21 Metabolism-Dependent Background Labeling of Proteins but Are Generally Reliable  
22 Tools for the Identification of Glycoproteins. *Front Chem* **8**, 529502 (2020).

23 37. Daughtry, J. L., Cao, W., Ye, J. & Baskin, J. M. Clickable Galactose Analogues for  
24 Imaging Glycans in Developing Zebrafish. *ACS Chem Biol* **15**, 318–324 (2020).

25 38. Beahm, B. J. *et al.* A visualizable chain-terminating inhibitor of glycosaminoglycan  
26 biosynthesis in developing zebrafish. *Angew Chem Int Ed Engl* **53**, 3347–3352  
27 (2014).

28 39. Bakker, H. *et al.* Functional UDP-xylose transport across the endoplasmic  
29 reticulum/golgi membrane in a Chinese hamster ovary cell mutant defective in UDP-  
30 xylose synthase. *J Biol Chem* **284**, 2576–2583 (2009).

31 40. Cioce, A. *et al.* Cell-specific bioorthogonal tagging of glycoproteins. *Nat Commun* **13**,  
32 1–18 (2022).

33 41. Cioce, A., Malaker, S. A. & Schumann, B. Generating orthogonal glycosyltransferase  
34 and nucleotide sugar pairs as next-generation glycobiology tools. *Curr Opin Chem*  
35 *Biol* **60**, 66–78 (2021).

36 42. Schumann, B. *et al.* Bump-and-Hole Engineering Identifies Specific Substrates of  
37 Glycosyltransferases in Living Cells. *Mol Cell* **78**, 824–834.e15 (2020).

38 43. Gao, J. *et al.* Exploration of Human Xylosyltransferase for Chemoenzymatic Synthesis  
39 of Proteoglycan Linkage Region. *Org Biomol Chem* **19**, 3374–3378 (2021).

40 44. Calle, B. *et al.* Benefits of Chemical Sugar Modifications Introduced by Click  
41 Chemistry for Glycoproteomic Analyses. *J Am Soc Mass Spectrom* **32**, 2366–2375  
42 (2021).

43 45. von Marschall, Z. & Fisher, L. W. Decorin is processed by three isoforms of bone  
44 morphogenetic protein-1 (BMP1). *Biochem Biophys Res Commun* **391**, 1374–1378  
45 (2010).

46 46. Seo, N. S., Hocking, A. M., Höök, M. & McQuillan, D. J. Decorin Core Protein  
47 Secretion Is Regulated by N-Linked Oligosaccharide and Glycosaminoglycan  
48 Additions. *J Biol Chem* **280**, 42774–42784 (2005).

49 47. Cioce, A. *et al.* Optimization of Metabolic Oligosaccharide Engineering with  
50 Ac4GalNAlk and Ac4GlcNAlk by an Engineered Pyrophosphorylase. *ACS Chem Biol*  
51 **16**, 1961–1967 (2021).

52 48. Führing, J. I. *et al.* A Quaternary Mechanism Enables the Complex Biological  
53 Functions of Octameric Human UDP-glucose Pyrophosphorylase, a Key Enzyme in  
54 Cell Metabolism. *Sci Rep* **5**, 1–11 (2015).

1 49. Yu, S. H. *et al.* Metabolic labeling enables selective photocrosslinking of O-GlcNAc-  
2 modified proteins to their binding partners. *Proc Natl Acad Sci U S A* **109**, 4834–4839  
3 (2012).

4 50. Murphy, L. D. *et al.* Synthesis of biolabile thioalkyl-protected phosphates from an  
5 easily accessible phosphotriester precursor. *Chem Sci* **14**, 5062–5068 (2023).

6 51. Mehellou, Y., Rattan, H. S. & Balzarini, J. The ProTide Prodrug Technology: From the  
7 Concept to the Clinic. *J Med Chem* **61**, 2211–2226 (2018).

8 52. Guinan, M., Huang, N., Smith, M. & Miller, G. J. Design, chemical synthesis and  
9 antiviral evaluation of 2'-deoxy-2'-fluoro-2'-C-methyl-4'-thionucleosides. *Bioorg Med  
10 Chem Lett* **61**, 128605 (2022).

11 53. Morozzi, C. *et al.* Targeting GNE Myopathy: A Dual Prodrug Approach for the Delivery  
12 of N-Acetylmannosamine 6-Phosphate. *J Med Chem* **62**, 8178–8193 (2019).

13 54. McGuigan, C. *et al.* Phosphate prodrugs derived from N-acetylglucosamine have  
14 enhanced chondroprotective activity in explant cultures and represent a new lead in  
15 antiosteoarthritis drug discovery. *J Med Chem* **51**, 5807–5812 (2008).

16 55. Ross, B. S., Ganapati Reddy, P., Zhang, H. R., Rachakonda, S. & Sofia, M. J.  
17 Synthesis of diastereomerically pure nucleotide phosphoramidates. *J Org Chem* **76**,  
18 8311–8319 (2011).

19 56. Barnett, M. W., Fisher, C. E., Perona-Wright, G. & Davies, J. A. Signalling by glial cell  
20 line-derived neurotrophic factor (GDNF) requires heparan sulphate  
21 glycosaminoglycan. *J Cell Sci* **115** 4495–4503 (2002).

22 57. Sterner, E., Meli, L., Kwon, S. J., Dordick, J. S. & Linhardt, R. J. FGF-FGFR signaling  
23 mediated through glycosaminoglycans in microtiter plate and cell-based microarray  
24 platforms. *Biochemistry* **52**, 9009–9019 (2013).

25 58. Götting, C., Kuhn, J. & Kleesiek, K. Human xylosyltransferases in health and disease.  
26 *Cell Mol Life Sci* **64**, 1498–1517 (2007).

27 59. Maciej-hulme, M. L. *et al.* Selective inhibition of heparan sulphate and not chondroitin  
28 sulphate biosynthesis by a small, soluble competitive inhibitor. *Int J Mol Sci* **22**, 6988  
29 (2021).

30 60. O'Leary, T. R. *et al.* Chemical editing of proteoglycan architecture. *Nat Chem Biol* **18**,  
31 634–642 (2022).

32 61. Batt, A. R., Zaro, B. W., Navarro, M. X. & Pratt, M. R. Metabolic Chemical Reporters  
33 of Glycans Exhibit Cell-Type-Selective Metabolism and Glycoprotein Labeling.  
34 *ChemBioChem* **18**, 1177–1182 (2017).

35